The Benefits of Respiratory Gating in ^{18}F-FDG PET Imaging of the Liver

Joël Daouk[1,2], Loïc Fin[3], Pascal Bailly[1], Jérôme Slama[1], Momar Diouf[3], Julie Morvan[1,2], Isabelle El Esper[1,2], Jean-Marc Régimbau[2,4], Denis Chatelain[2,5], Marc-Etienne Meyer[1,2]

[1]Department of Nuclear Medicine, [2]Faculty of Medicine, Jules Verne University of Picardy,

[3]Clinical Trial and Innovation Department, [4]Department of Visceral and Digestive Surgery,

[5]Department of Pathology, Amiens University Hospital, Amiens, France

bailly.pascal@chu-amiens.fr

***Abstract*-In ^{18}F-fluorodeoxyglucose (^{18}F-FDG) positron emission tomography/computed tomography (PET/CT), respiratory motion induces bias in image interpretations. This issue has been widely discussed at the thoracic level. However, although liver is also affected by physiological motion, it has not been well investigated yet. This study assessed the application of a custom gating method (referred to as the "CT-based gated PET") to PET imaging of the liver and evaluated its benefits in terms of per-lesion sensitivity over ungated clinical PET images. 30 patients scheduled for hepatic surgery were referred to our department for PET/CT imaging. Each patient underwent both ungated and CT-based gated PET imaging protocols. The blinded image interpretations were combined with histological analysis and intra-operative ultrasound to compute each method's per-lesion sensitivity and positive predictive value (PPV). 74 lesions were confirmed by pathology reports. When considering all the uptakes, ungated and CT-based gated PET sensitivities were 64% and 73%, with PPVs of 82% and 75%, respectively. Our CT-based gated PET method showed a higher lesion-based sensitivity than routine, ungated examination did, although it yielded a higher proportion of false positive descriptions. The gain in sensitivity was due to the detection of lesions of between 15 and 25mm in size in gated PET images. Hence, accurate respiratory motion compensation should be implemented in order to improve the diagnosis, staging and follow-up of liver cancer.**

Keywords-PET/CT; ^{18}F-fluorodeoxyglucose; Liver Cancer; Respiratory Motion

I. INTRODUCTION

^{18}F-fluorodeoxyglucose (^{18}F-FDG) positron emission tomography/computed tomography (PET/CT) has become a major imaging modality for the management of patients with suspected liver cancer [1, 2]; this is notably because of the technique's ability to detect distant metastases. Hepatic resection is known to be the only curative treatment in a subset of liver cancer patients. Eligibility for hepatic surgery is based on conventional staging, including contrast-enhanced CT, magnetic resonance imaging or ultrasonography of the liver [2, 3]. Recently, ^{18}F-FDG PET/CT was introduced as a staging modality in the preoperative work-up for hepatic surgery of colorectal liver metastases [4]. However, many physiological issues can affect the accuracy of PET images and thus their interpretation. Indeed, the physician can miss lesions on the ^{18}F-FDG PET/CT images due to particular histologies (e.g. in moderate or well-differentiated hepatocellular carcinoma (HCC) [5] or mucinous carcinoma [6]). Conversely, local inflammation is sometimes wrongly interpreted as a malignant lesion [7].

Another issue in PET imaging of the liver is respiratory motion, which produces blurring in reconstructed images [8, 9] and can cause some lesions to be missed or underestimated. The motion issue is well known in thoracic imaging and a variety of compensation methods have been suggested. This kind of respiratory-gated PET technique (amplitude- or phase-based methods) divides the respiratory signal and the acquired PET data into several frames [10-12]. The main drawback of this strategy is that several PET volumes are attenuation-corrected with the same CT-derived attenuation map. Thus, the quantification problem is not solved and PET-to-CT lesion co-localization remains uncertain [10].

Nehmeh et al. [13] suggested performing both PET and CT acquisitions during a deep-inspiration breath-hold. For the PET examination, 20-second episodes of apnoea were repeated several times, so as to recover enough counting statistics. However, repetition of these apnoeic periods can be stressful and tiring - especially for dyspnoeic patients.

We have suggested a motion compensation technique (referred to hereafter as the "CT-based gated PET" method) in which a single PET volume is generated by selecting appropriate events from a respiratory-gated PET acquisition (performed in free-breathing) with respect to a single, short, breath-hold CT acquisition (BH-CT) [14, 15].

To the best of our knowledge, only one study has assessed respiratory-gated PET acquisition for abdominal staging [16]. However, the group did not perform a sensitivity study to assess the usefulness of gated acquisitions in term of lesion detection. The goal of the clinical trial presented here was to apply our CT-based gated PET method to the liver and then compare its per-lesion sensitivity with that of PET images acquired with a standard clinical protocol (referred to here as the "ungated" method).

II. MATERIALS AND METHODS

A. Patients

TABLE I PATIENT CHARACTERISTICS

Characteristic	Data
Gender (n)	
Male	21
Female	9
Age (y) (mean; range)	60; 32 – 81
Body mass index (mean; range)	26; 20 – 36
Glucose blood level (g/L) (mean; range)	1.0; 0.6 – 2.9
Injected activity (MBq) (mean; range)	376.5; 278.0 – 513.0

Between October 2008 and December 2009, 30 patients were prospectively enrolled in this single-centre study at Amiens University Hospital. The inclusion criteria were (i) the indication of hepatic resection for the removal of primary or metastatic hepatic lesions and (ii) a preoperative PET/CT examination. The study population's characteristics are summarized in Table I.

The study was approved by the local independent ethics committee and all patients provided written, informed consent to participation (ClinicalTrials.gov identifier: NCT01219985).

B. PET/CT Acquisitions

After fasting for at least 6 hours and verification of a normal glucose blood level, each patient received an intravenous injection of ^{18}F-FDG. After a 60-minute uptake phase in a quiet environment, patients underwent the PET/CT examination.

All acquisitions were performed on a whole-body PET/CT system (HiRez Biograph™ 6, Siemens Medical Solutions) equipped with lutetium oxyorthosilicate crystals, each of which measures 4 mm x 4 mm x 20 mm and was integrated into a 13 x 13 detector block. The system has axial and transaxial fields of view measuring 162 and 585 mm, respectively [17]. The spiral CT scanner (Emotion 6; Siemens Medical Solutions) is a 6-slice machine with a slice thickness ranging from 0.63 to 10 mm. A 360 ° source rotation takes 0.6 s.

1) Whole-Body PET/CT (The Ungated Session)

The ungated acquisition consisted in a whole-body, free-breathing CT acquisition (tube voltage: 110 kV; reference tube current:

85mAs; pitch: 1) followed by a standard multistep PET acquisition (3 minutes per step), as used in routine clinical practice in our Department.

2) CT-Based Gated PET Session

It consisted in the addition of an extra step at the end of the ungated session: a 10-minute list mode respiratory-gated PET acquisition (RG-PET) followed by a 7-second end-expiration breath-hold CT acquisition (tube voltage: 110 kV; reference tube current: 50 mAs; pitch: 2), with continuous respiratory signal recording. Respiratory gating was performed with the AZ733V system (Anzai Medical, 126 Tokyo, Japan), which measures the abdominal wall pressure. The event selection methodology has been fully described in Fin et al. [15]. In brief, the breath-hold CT sequence is visible on the respiratory signal as a plateau. A selection range is placed around this plateau to select only those PET events emitted when tissues were in the same position as in the breath-hold CT (Fig. 1).

In the following text, the ungated dataset refers to the PET and CT data acquired in free-breathing mode and corresponding to the bed position of the respiratory-gated session. The CT-based gated PET dataset refers to PET and CT data acquired and processed during the CT-based gated PET session.

C. Image Reconstruction

After the compensation for random coincidences, all 3-dimensional sinograms were FORE-rebinned [18] into two dimensions and scatter-corrected [19]. The attenuation coefficients at 511 keV were calculated from the CT acquisition, in order to correct for tissue attenuation [20]. Ungated volumes were corrected with the free-breathing CT scan and CT-based gated PET volumes were corrected with the end-expiration, breath-hold CT. All PET volumes were reconstructed using AW-OSEM [21] with the following parameters: 4 iterations, 8 ordered subsets with 168 x 168 x 81 matrices (4.06 mm x 4.06 mm x 2 mm). Lastly, a 3-dimensional isotropic Gaussian post-filter with a full width at half maximum of 5 mm was applied to each volume.

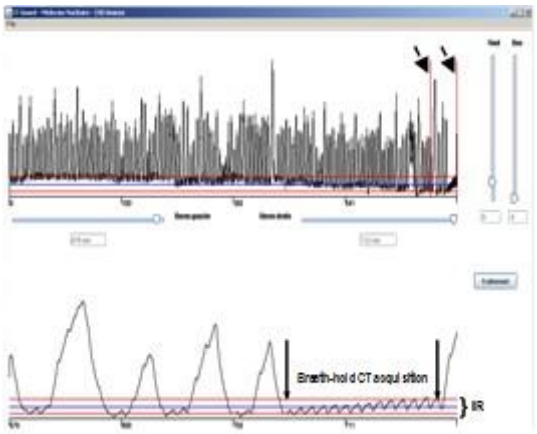

Fig. 1 CT-based processing home-made Java application. The upper part of the figure shows the entire respiratory signal of a patient. Lower part presents a zoomed portion of the respiratory signal. This portion was defined by the two vertical bars (see dashed arrows). A selection range (SR) was placed around breath-hold computed tomography (CT) respiratory trace to select PET events which occurred at the same tissues positions than breath-hold CT acquisition.

D. Image Analysis

Each PET examination was blindly and independently analysed by two experienced nuclear medicine physicians; neither the type of image (i.e. ungated or CT-based gated PET images) nor the patient's information was known to the observers. Each observer had to report the number of lesions detected respectively in the ungated and CT-based gated PET datasets and then specify (i) each lesion's location on a schematic representation of the liver segments (according to the Couinaud segmental classification) and (ii) the lesion's maximum standardized uptake value (SUVmax).

E. Surgical Procedure and Histopathological Analysis

Intra-operative ultrasound was always performed, in order to detect and localize all liver lesions. The surgeon aimed at obtaining disease-free resection margins. The type of liver resection (hepatectomy or wedge resection) and the use or not of radiofrequency tumour ablation was left to the surgeon's discretion. Lesion sites were noted by the surgeon on a large-scale diagram of the liver, as the gold standard for the tumour’s location.

When available, pathological examination of surgical specimens was performed to assess the tumour's size, its distance to the surgical margins and its histological subtype and differentiation stage.

F. Database Construction

Histopathological and intra-operative ultrasound reports were combined with PET interpretations to build a lesion

database. A "lesion sheet" was created if either an uptake was described by at least one observer for at least one method and/or a lesion was identified during pathological analysis or (by default) by intra-operative ultrasound examination. Each lesion sheet contained five fields: (i) two "image interpretation fields" for observer 1 (one for ungated and one for CT-based gated PET) (ii) two image interpretation fields for observer 2 (one for each method) and (iii) one "malignancy field".

The image interpretation field was set to "1" if the considered uptake was identified by a given observer with a given method. If not, the field was set to "0". Likewise, the malignancy field was set to "1" if the pathology report and/or intra-operative ultrasound reported this lesion. If not, the field was set to "0".

Next, for each lesion sheet, a rating score (RS) (0-2 points) was attributed to each method by adding up the respective image interpretation field values. This score reflected the observers' degree of agreement (0: agreement, non-visible; 1: disagreement; 2: agreement, visible). This RS was not checked against the result of the pathology report.

TABLE II THE LESION CLASSIFICATION METHOD FOR THE BROAD STRATEGY

Malignancy field	Rating score		
	0	1	2
1	FN	TP	TP
0	TN	FP	FP
FN: false negative; TP: true positive; TN: true negative; FP: false positive			

TABLE III THE LESION CLASSIFICATION METHOD FOR THE STRICT STRATEGY

Malignancy field	Rating score		
	0	1	2
1	FN	FN	TP
0	TN	TN	FP
FN: false negative; TP: true positive; TN: true negative; FP: false positive			

G. Statistical Analysis

We calculated ungated and CT-based gated PET sensitivities and positive predictive value (PPV) according to a broad strategy (BS) and a strict strategy (SS). In the BS, uptakes with an RS of 1 or 2 were considered to be potential lesions. In the SS, only uptakes with an RS of 2 were considered to be potential lesions. The classification methods for the BS and SS are depicted in Tables II and III, respectively.

Specificity could not be calculated because the presence of liver disease was an inclusion criterion. In addition, this was a lesion-based study and it was impossible to compute the true negative component of the contingency table.

The inter-observer variability for all lesions was assessed by applying Cohen's Kappa test to the observers' reports. We performed a McNemar test to compare the sensitivities obtained for each method and with each strategy. A p value of less than 0.05 was considered to be statistically significant.

As a secondary outcome measure, we compared the SUV_{max} obtained with ungated and CT-based gated PET methods, respectively, after having checked that the values were normally distributed.

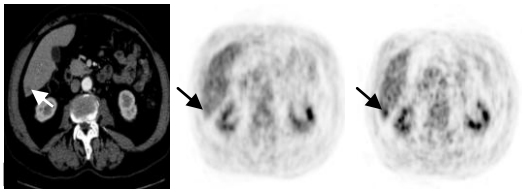

(a) (b) (c)

Fig. 2 Patient 24 presented a suspect lesion (see arrow) in segment VI on a contrast-enhanced CT image (a). On the ungated transverse image (b), the observers did not identify any uptake in this location (see arrow). The CT-based gated PET image (c) revealed focal uptake (see arrow; maximum standardized uptake value: 5.2). Pathological analysis confirmed the presence of a synchronous liver metastasis of a rectal carcinoma

III. RESULTS

Table IV summarizes the histopathological reports on the 30 patients who underwent surgery. The mean time interval between PET examination and surgery was 34 days (range: 1 to 249 days).

TABLE IV HISTOLOGICAL RESULTS

Histological result	Patients (n)
Liver metastasis of colorectal carcinoma	18
Moderately differentiated hepatocellular carcinoma	3
Well-differentiated hepatocellular carcinoma	2
Cholangiocarcinoma	1
Liver metastasis of endocrine carcinoma	2
Liver metastasis of breast carcinoma	2
Liver metastasis of ovarian carcinoma	1
Benign lesion (acute cholecystitis with liver abscess)	1

Seventy-four intrahepatic lesions were identified in 30 patients with a histological and/or intraoperative ultrasound analysis.

Fig. 2 presents PET images acquired with the ungated and CT-based gated PET methods for patient 24. In Fig. 2a, a suspect lesion is visible on the contrast-enhanced CT image (see the arrow). On the corresponding ungated PET image (Fig. 2b), the observers did not identify any uptake; the RS was therefore = 0. With the CT-based gated PET image (Fig. 2c), the observers described a lesion (SUV_{max} = 5.2) in segment VI, at the location corresponding to the suspect lesion seen on the CT image in Fig. 2a. Accordingly, the RS for this lesion was equal to 2. After liver resection of segment VI, pathological analysis confirmed the presence of a synchronous liver metastasis of a rectal carcinoma.

Table V presents sensitivity and PPV results for the BS and SS with ungated and CT-based gated PET data. In both strategies, CT-based gated PET sensitivity was higher than that of the ungated method (14.8% and 5.0% higher for the BS and SS, respectively). The PPV was lower in the CT-based gated PET than in the ungated method (a decrease of 8.5% and 2.3% for the BS and SS, respectively).

A McNemar test revealed a significant difference between CT-based gated PET and ungated methods in the BS ($p<0.001$) but not in the SS.

According to the Landis and Koch interpretation of Cohen's Kappa [22], the inter-observer agreement was almost

perfect with the ungated method (=084) but only moderate with CT-based gated PET (=057).

Lastly, only lesions which had an RS of 2 in both methods (i.e. to obtain paired samples) were selected to perform SUV_{max} study. The mean SUV_{max} (± SD) were 7.6 ± 3.1 and 8.5 ± 3.5 for ungated and CT-based gated PET methods, respectively. The normality test for SUV_{max} data in ungated and CT-based gated PET volumes revealed that both series were normally distributed. A two-tailed paired Student's t-test revealed a significant inter-method difference ($p<0.001$).

IV. DISCUSSION

The objective of this study was to assess the impact of a respiratory gating method on the detection of hepatic lesions in ^{18}F-FDG PET/CT images. Indeed, the liver is strongly affected by respiratory motion [8, 9, 23] and this situation can lead to a degree of misinterpretation. During normal breathing in the supine position, the liver moves by an average of 11 mm [9]. However, movements of up to 26 mm have been observed [24]. It is therefore reasonable to hypothesize that respiratory gating can improve the performance of PET/CT for the detection of liver lesions. Thus, one of the expected outcomes of this study was an improvement in per-lesion sensitivity via the application of our CT-based gated PET method.

TABLE V CONTINGENCY TABLE FOR THE UNGATED AND CT-BASED GATED PET METHODS. THE P VALUE IS THE RESULT OF MCNEMAR TEST WITH A 0.05 SIGNIFICANCE THRESHOLD

	Broad strategy		Strict strategy	
	Ungated	CT-based	Ungated	CT-based
TP	47	54	42	44
FN	27	20	32	30
FP	9	17	6	7
Sensitivity	64%	73%	57%	60%
p	<0.001		NS	
PPV	82%	75%	88%	86%
TP: true positive ; FN: false negative ; FP: false positive; PPV: positive predictive value ; NS: not significant				

The observed sensitivity values of this study for the ungated method are consistent with published similar series (ranging from 39% to 88%) [6, 25, 26]. However, these studies had specific inclusion criteria (tumour histology and size or the use of neoadjuvant therapy). To the best of our knowledge, only the study by Böhm et al. [27] includes both primary and secondary tumours. They obtained a sensitivity of 82% but did not describe the study population or the inclusion criteria. CT-based gated PET method, whatever the strategy used, led to an improvement in sensitivity over the ungated method (Table V).

In a previous paper, we showed that the CT-based gated PET method produced an accurate attenuation correction and thus provided more reliable SUV_{max} [15]. In the present study, SUV_{max} were significantly higher in CT-based gated PET images than in ungated images. This finding is consistent with a previously published paper dealing with the usefulness of respiratory gating in abdominal PET imaging [16].

There were several false negative lesions in our present study. Indeed, a limitation of our study relates to the diversity of the clinical situations considered (secondary and primary tumours, neoadjuvant chemotherapy, etc.). Thus, factors other than respiratory motion (tumour histology and size, the use of chemotherapy, etc.) may have affected the performance of our results. This situation may explain (at least in part) the relatively low per-lesion sensitivity found here.

In terms of colorectal liver metastases, it is known that the low cellularity of mucinous adenocarcinomas makes ^{18}F-FDG PET/CT less sensitive [6]. In our series, three lesions not reported by the two observers (RS = 0) in either method had a major mucinous component. Moreover, the sensitivity of ^{18}F-FDG PET/CT for HCC is known to be low (between 50% and 60%) [28]. Indeed, unlike most malignancies, HCC does not strongly express the GLUT 1 glucose transporter [29] and thus is not avid for ^{18}F-FDG (especially in the case of well-differentiated HCC) [30]. This explains why the two well-differentiated HCC tumours in our series were not reported, whatever the observer or the method.

In addition, well-differentiated endocrine tumours have the same, low ^{18}F-FDG avidity as HCC [31]. In our study, two lesions not reported by the observers in either method were well-differentiated endocrine tumours.

Lesion size is also a major concern in lesion detection with PET/CT. Given the low spatial resolution in PET (about 5 mm for our tomograph [17]), hepatic lesions with a greatest dimension below 15 mm (i.e. two to three times the PET system's spatial resolution) are hardly detectable [32]. In a PET study of colorectal carcinoma metastases, Delbeke et al. improved the sensitivity from 91% to 99% by excluding lesions smaller than 10 mm [33]. Similarly for HCC, Park et al. have clearly demonstrated the influence of lesion size on ^{18}F-FDG PET/CT sensitivity (27.2% for lesions 10 to 20 mm in size and 92.8% for those greater than or equal to 50 mm in size) [28]. In the present work, 19 lesions less than or equal to 15 mm in greatest dimension were not identified by the observers on ungated and CT-based gated PET images. Application of CT-based gated PET increased the RS for 10 malignant lesions (from "0" to "1" for seven lesions and from "1" to "2" for three lesions), compared with the ungated method. Nine of these were smaller than 25 mm - showing that not compensating for respiratory motion worsens the contrast of these lesions and may render them invisible.

Interpretation of PET images of the liver is highly subjective and thus highly sensitive to inter-observer variability. Classically, this issue has been resolved by consensus. However, use of a consensus method prevents the analysis of inter-observer variability. In the present study, we decided to analyse two combinations of the results provided by two different observers. In the BS, any lesion with an RS greater than 0 was considered to be positive (without taking pathological results into account). This strategy mimicked a pseudo-observer who would describe any uptake as a potential lesion. In contrast, the SS considered only uptakes for which agreement was obtained from the two observers to be positive. As such, it mimicked an observer who would tend to describe only the most obvious uptakes. Most observers would fall between these two extreme behaviours in terms of sensitivity and PPV (Table V). For example, the sensitivity results for observer 1 were 62% and 64% (with PPVs of 87% and 86%) for the ungated and CT-based gated PET methods, respectively. For observer 2, the sensitivities were 58% and 69% (with PPVs of 84% and 76%) for ungated and CT-based gated PET methods, respectively. In all cases, we noted that our CT-based gated PET method provided higher sensitivity

than the ungated method did. However, this improvement was accompanied by an increase in the number of false positives (FPs); furthermore, the size of the increase depended on the strategy employed. This is reflected by the respective PPVs: 75% and 82% for CT-based gated PET and ungated PET when using the BS and 86% and 88% when using the SS (Table V)). The main reason for the high proportion of FPs obtained with the CT-based gated PET method in BS was probably inter-observer variability. Indeed, most of CT-based gated PET FPs had an RS of 1, indicating disagreement between the observers' interpretations (as highlighted by the lower □). This can be attributedto noise or the liver's intrinsic heterogeneity. In ungated images, these foci are blurred by respiratory motion and are thus less likely to be reported. Removing the motion component restores these heterogeneities.

There are many possible explanations for the heterogeneities and non-malignant uptakes observed on liver PET images. Some of our patients underwent chemo-embolization shortly before their PET examination. This may have induced some CT artefacts which in turn could have altered the attenuation maps and introduced bias in PET images. This was the case for one patient (patient 31) for whom both observers identified three uptakes on the ungated volume and four uptakes on the CT-based gated volume, whereas no lesion was reported by intra-operative ultrasound examination.

According to literature reports, adjuvant chemotherapy or radiofrequency ablation can produce false positive results [34]. Indeed, it has been shown that ^{18}F-FDG accumulates significantly more in inflammatory tissue than it does in normal tissue [7]. However, the extent of accumulation in inflammatory lesions is lower than in tumours. Respiratory motion (which lowers contrast) can render these uptakes invisible. Five to eight of the FPs can be explained by this phenomenon. Two other FPs were described in a cirrhotic liver in a patient with hepatitis C. These foci may result from the virosis-related inflammation or may correspond to the regenerative nodules often observed in this disease [35].

The event selection range was defined so that it contained around 20% to 25% of the mean amplitude of a given patient's respiratory signal. The mean event selection range (± SD) was 23±10%, corresponding to selection of 27±7% of the total counting statistics (also corresponding to 162±42s).

The CT-based gated PET method may have some implications in a clinical setting, notably when patients are addressed for the staging of cancers which are suspected to spread to the liver (e.g. colorectal carcinoma, ductal carcinoma, etc.). The CT-based gated PET method allowed the detection of more lesions than the ungated method did; this difference may alter patient management practices. However, clinicians should be cautious when describing additional uptakes on synchronized images, in view of the high number of false positives. One way of avoiding this type of over-description could be the use of contrast-enhanced breath-hold CT during the CT-based gated PET session. Indeed, it has been shown that CT contrast agents and PET tracers are complementary in combined PET/CT imaging, notably for the liver [36]. Another solution for resolving non-malignant uptakes could be a computer-aided decision support tool. Given that noise in liver parenchyma does not have the same pattern as a lesion; it should be possible to discriminate between real foci and noisy uptakes. Our group is currently investigating this type of algorithm.

V. CONCLUSION

Our CT-based gated PET method showed a higher lesion-based sensitivity than routine, ungated examination did. The gain in sensitivity was due to the detection of lesions of between 15 and 25 mm in size in gated PET images - lesions that go unseen in ungated images. However, as with any respiratory-gated method, the CT-based gated PET method requires a relatively steady respiratory signal. The removal of motion blurring restores the liver's intrinsic heterogeneity and can induce over-interpretations.

ACKNOWLEDGMENT

The authors wish to thank Dr David Fraser (Biotech Communication, Damery, France) for his helpful advice on the English language in this paper.

The authors thank Dr Véronique Moullart, Dr Lazhar Saidi and the Nuclear Medicine Department's technologists for their advice on and valuable help with the acquisition of the data used in the present study.

REFERENCES

[1] S. C. Chua, A. M. Groves, I. Kayani, L. Menezes, S. Gacinovic, Y. Du, J. B. Bomanji, and P. J. Ell, "The impact of 18F-FDG PET/CT in patients with liver metastases," Eur J Nucl Med Mol Imaging, vol. 34, pp. 1906-14, Dec 2007.

[2] M. R. Oliva and S. Saini, "Liver cancer imaging: role of CT, MRI, US and PET," Cancer Imaging, vol. 4 Spec No A, pp. S42-6, 2004.

[3] I. Floriani, V. Torri, E. Rulli, D. Garavaglia, A. Compagnoni, L. Salvolini, and A. Giovagnoni, "Performance of imaging modalities in diagnosis of liver metastases from colorectal cancer: a systematic review and meta-analysis," J Magn Reson Imaging, vol. 31, pp. 19-31, Jan 2010.

[4] T. J. Ruers, B. Wiering, J. R. van der Sijp, R. M. Roumen, K. P. de Jong, E. F. Comans, J. Pruim, H. M. Dekker, P. F. Krabbe, and W. J. Oyen, "Improved selection of patients for hepatic surgery of colorectal liver metastases with (18)F-FDG PET: a randomized study," J Nucl Med, vol. 50, pp. 1036-41, Jul 2009.

[5] Y. Yamamoto, Y. Nishiyama, R. Kameyama, K. Okano, H. Kashiwagi, A. Deguchi, M. Kaji, and M. Ohkawa, "Detection of hepatocellular carcinoma using 11C-choline PET: comparison with 18F-FDG PET," J Nucl Med, vol. 49, pp. 1245-8, Aug 2008.

[6] N. Lubezky, U. Metser, R. Geva, R. Nakache, E. Shmueli, J. M. Klausner, E. Even-Sapir, A. Figer, and M. Ben-Haim, "The role and limitations of 18-fluoro-2-deoxy-D-glucose positron emission tomography (FDG-PET) scan and computerized tomography (CT) in restaging patients with hepatic colorectal metastases following neoadjuvant chemotherapy: comparison with operative and pathological findings," J Gastrointest Surg, vol. 11, pp. 472-8, Apr 2007.

[7] T. Mochizuki, E. Tsukamoto, Y. Kuge, K. Kanegae, S. Zhao, K. Hikosaka, M. Hosokawa, M. Kohanawa, and N. Tamaki, "FDG uptake and glucose transporter subtype expressions in experimental tumor and inflammation models," J Nucl Med, vol. 42, pp. 1551-5, Oct 2001.

[8] Y. Nakamoto, M. Tatsumi, C. Cohade, M. Osman, L. T. Marshall, and R. L. Wahl, "Accuracy of image fusion of normal upper abdominal organs visualized with PET/CT," Eur J Nucl Med Mol Imaging, vol. 30, pp. 597-602, Apr 2003.

[9] P. H. Weiss, J. M. Baker, and E. J. Potchen, "Assessment of hepatic respiratory excursion," J Nucl Med, vol. 13, pp. 758-9, Oct 1972.

[10] J. Daouk, L. Fin, P. Bailly, and M. E. Meyer, "Respiratory-Gated Positron Emission Tomography and Breath-Hold Computed Tomography Coupling to Reduce the Influence of Respiratory Motion: Methodology and Feasibility," Acta Radiol, vol. 50, pp. 144-155, Dec 19 2009.

[11] M. Dawood, F. Buther, N. Lang, O. Schober, and K. P. Schafers, "Respiratory gating in positron emission tomography: a quantitative comparison of different gating schemes," Med Phys, vol. 34, pp. 3067-76, Jul 2007.

[12] G. Chang, T. Chang, T. Pan, J. W. Clark, Jr., and O. R. Mawlawi, "Implementation of an automated respiratory amplitude gating technique for PET/CT: clinical evaluation," J Nucl Med, vol. 51, pp. 16-24, Jan 2010.

[13] S. A. Nehmeh, Y. E. Erdi, G. S. Meirelles, O. Squire, S. M. Larson, J. L. Humm, and H. Schoder, "Deep-inspiration breath-hold PET/CT of the thorax," J Nucl Med, vol. 48, pp. 22-6, Jan 2007.

[14] J. Daouk, L. Fin, P. Bailly, and M. E. Meyer, "Improved attenuation correction via appropriate selection of respiratory-correlated PET data," Comput Methods Programs Biomed, vol. 92, pp. 90-8, Oct 2008.

[15] L. Fin, J. Daouk, J. Morvan, P. Bailly, I. El Esper, L. Saidi, and M. E. Meyer, "Initial clinical results for breath-hold CT-based processing of respiratory-gated PET acquisitions," Eur J Nucl Med Mol Imaging, vol. 35, pp. 1971-80, Nov 2008.

[16] S. Nagamachi, H. Wakamatsu, S. Kiyohara, S. Fujita, S. Futami, H. Arita, R. Nishii, S. Tamura, and K. Kawai, "Usefulness of a deep-inspiration breath-hold 18F-FDG PET/CT technique in diagnosing liver, bile duct, and pancreas tumors," Nucl Med Commun, vol. 30, pp. 326-32, May 2009.

[17] M. Brambilla, C. Secco, M. Dominietto, R. Matheoud, G. Sacchetti, and E. Inglese, "Performance characteristics obtained for a new 3-dimensional lutetium oxyorthosilicate-based whole-body PET/CT scanner with the National Electrical Manufacturers Association NU 2-2001 standard," J Nucl Med, vol. 46, pp. 2083-91, Dec 2005.

[18] M. Defrise, P. E. Kinahan, D. W. Townsend, C. Michel, M. Sibomana, and D. F. Newport, "Exact and approximate rebinning algorithms for 3-D PET data," IEEE Trans Med Imaging, vol. 16, pp. 145-58, Apr 1997.

[19] C. C. Watson, "New, faster, image-based scatter correction for 3D PET," IEEE Transactions on Nuclear Science, vol. 47, pp. 1587-1594, aug 2000.

[20] P. E. Kinahan, D. W. Townsend, T. Beyer, and D. Sashin, "Attenuation correction for a combined 3D PET/CT scanner," Med Phys, vol. 25, pp. 2046-53, Oct 1998.

[21] C. Comtat, P. E. Kinahan, M. Defrise, C. Michel, and D. W. Townsend, "Fast reconstruction of 3D PET data with accurate statistical modeling," IEEE Transactions on Nuclear Science, vol. 45, pp. 1083-1089, Jun 1998.

[22] J. R. Landis and G. G. Koch, "The measurement of observer agreement for categorical data," Biometrics, vol. 33, pp. 159-74, Mar 1977.

[23] W. V. Vogel, J. A. van Dalen, B. Wiering, H. Huisman, F. H. Corstens, T. J. Ruers, and W. J. Oyen, "Evaluation of Image Registration in PET/CT of the Liver and Recommendations for Optimized Imaging," J Nucl Med, vol. 48, pp. 910-9, Jun 2007.

[24] M. A. Clifford, F. Banovac, E. Levy, and K. Cleary, "Assessment of hepatic motion secondary to respiration for computer assisted interventions," Comput Aided Surg, vol. 7, pp. 291-9, 2002.

[25] C. Carnaghi, M. C. Tronconi, L. Rimassa, L. Tondulli, M. Zuradelli, M. Rodari, R. Doci, F. Luttmann, G. Torzilli, D. Rubello, A. Al-Nahhas, A. Santoro, and A. Chiti, "Utility of 18F-FDG PET and contrast-enhanced CT scan in the assessment of residual liver metastasis from colorectal cancer following adjuvant chemotherapy," Nucl Med Rev Cent East Eur, vol. 10, pp. 12-5, 2007.

[26] E. D. Rappeport, A. Loft, A. K. Berthelsen, P. von der Recke, P. N. Larsen, A. M. Mogensen, A. Wettergren, A. Rasmussen, J. Hillingsoe, P. Kirkegaard, and C. Thomsen, "Contrast-enhanced FDG-PET/CT vs. SPIO-enhanced MRI vs. FDG-PET vs. CT in patients with liver metastases from colorectal cancer: a prospective study with intraoperative confirmation," Acta Radiol, vol. 48, pp. 369-78, May 2007.

[27] B. Bohm, M. Voth, J. Geoghegan, H. Hellfritzsch, A. Petrovich, J. Scheele, and D. Gottschild, "Impact of positron emission tomography on strategy in liver resection for primary and secondary liver tumors," J Cancer Res Clin Oncol, vol. 130, pp. 266-72, May 2004.

[28] J. W. Park, J. H. Kim, S. K. Kim, K. W. Kang, K. W. Park, J. I. Choi, W. J. Lee, C. M. Kim, and B. H. Nam, "A prospective evaluation of 18F-FDG and 11C-acetate PET/CT for detection of primary and metastatic hepatocellular carcinoma," J Nucl Med, vol. 49, pp. 1912-21, Dec 2008.

[29] J. D. Lee, W. I. Yang, Y. N. Park, K. S. Kim, J. S. Choi, M. Yun, D. Ko, T. S. Kim, A. E. Cho, H. M. Kim, K. H. Han, S. S. Im, Y. H. Ahn, C. W. Choi, and J. H. Park, "Different glucose uptake and glycolytic mechanisms between hepatocellular carcinoma and intrahepatic mass-forming cholangiocarcinoma with increased (18)F-FDG uptake," J Nucl Med, vol. 46, pp. 1753-9, Oct 2005.

[30] J. Trojan, O. Schroeder, J. Raedle, R. P. Baum, G. Herrmann, V. Jacobi, and S. Zeuzem, "Fluorine-18 FDG positron emission tomography for imaging of hepatocellular carcinoma," Am J Gastroenterol, vol. 94, pp. 3314-9, Nov 1999.

[31] T. Binderup, U. Knigge, A. Loft, J. Mortensen, A. Pfeifer, B. Federspiel, C. P. Hansen, L. Hojgaard, and A. Kjaer, "Functional imaging of neuroendocrine tumors: a head-to-head comparison of somatostatin receptor scintigraphy, 123I-MIBG scintigraphy, and 18F-FDG PET," J Nucl Med, vol. 51, pp. 704-12, may 2010.

[32] E. J. Hoffman, S. C. Huang, D. Plummer, and M. E. Phelps, "Quantitation in positron emission computed tomography: 6. effect of nonuniform resolution," J Comput Assist Tomogr, vol. 6, pp. 987-99, Oct 1982.

[33] D. Delbeke, J. V. Vitola, M. P. Sandler, R. C. Arildsen, T. A. Powers, J. K. Wright, Jr., W. C. Chapman, and C. W. Pinson, "Staging recurrent metastatic colorectal carcinoma with PET," J Nucl Med, vol. 38, pp. 1196-201, Aug 1997.

[34] J. W. Lim, C. L. Tang, and G. H. Keng, "False positive F-18 fluorodeoxyglucose combined PET/CT scans from suture granuloma and chronic inflammation: report of two cases and review of literature," Ann Acad Med Singapore, vol. 34, pp. 457-60, Aug 2005.

[35] K. Yu, S. J. Schomisch, V. Chandramouli, and Z. Lee, "Hexokinase and glucose-6-phosphatase activity in woodchuck model of hepatitis virus-induced hepatocellular carcinoma," Comp Biochem Physiol C Toxicol Pharmacol, vol. 143, pp. 225-31, Jun 2006.

[36] G. Antoch, L. S. Freudenberg, T. Beyer, A. Bockisch, and J. F. Debatin, "To enhance or not to enhance? 18F-FDG and CT contrast agents in dual-modality 18F-FDG PET/CT," J Nucl Med, vol. 45 Suppl 1, pp. 56S-65S, Jan 2004.